Mobility of a reptating polymer with fast diffusion of stored length

Jan A. Leegwater* and J. M. J. van Leeuwen
Instituut-Lorentz, Rijksuniversiteit te Leiden, P.O. Box 9506, 2300 RA Leiden, The Netherlands
(Received 7 November 1994)

We study a reptation model of polymer electrophoresis in which the diffusion of stored length is very fast compared to the end point model. For long chains we find that the polymer becomes stretched. We demonstrate that the drift velocity in one dimension is higher by a factor 10/3 than would have been expected on the basis of simple estimates. This is caused by the fact that a polymer segment, once created, has a probability of staying that depends on its orientation. The scaling parameter determining the long chain behavior is $N\epsilon^2$, where N is proportional to the length of the polymer and ϵ is the (dimensionless) electric field strength. When $N\epsilon^2 \gtrsim 8$ the drift velocity becomes independent on the length of the polymer. For low fields we demonstrate that there is a crossover from a regime where the field can essentially be neglected to a regime where the field significantly changes the dynamics of the polymer. The scaling parameter determining this crossover is shown to be $N^3\epsilon^2$.

PACS number(s): 36.20.Ey, 82.45.+z, 05.40.+j

I. INTRODUCTION

Reptation as a model for polymer motion is well established [1,2]. It shows up for instance in gel electrophoresis for which we consider a model closely similar to the model introduced by Rubinstein [3] and modified by Duke [4]. The polymer is modeled as a chain of N particles that we will call reptons. These reptons move according to certain rules. The reptons are allowed to move on a d dimensional cubic lattice. We simulate only the one dimensional projection along the electric field since the dimension only modifies some numerical constants, but, as long as the reptons are noninteracting, no qualitative features. There are two different sorts of moves that we call internal moves and external moves, as illustrated in Fig. 1. The internal moves effect the diffusion of stored length (reptation) as introduced by de Gennes [1]. The external moves change the shape of the polymer, and these are the *only* moves to change the shape. The rates of the moves are dependent on the electric field, moves with the field having rates $W_{i,e}\exp(\epsilon/2)$, where i and e denote internal, and external, respectively. Moves against the field are less likely to occur, and have rates $W_{i,e}\exp(-\epsilon/2)$. In these expressions, ϵ is the field in dimensionless units, i.e.,

$$\epsilon = \frac{qEa}{k_B T} , \tag{1}$$

where q is the charge, a is the lattice spacing, E is the magnitude of the applied field, T is the temperature, and k_B is the Boltzmann constant. Perhaps the clearest definition of the model is given in Fig. 1; for a discussion of the physical approximations made, we refer to the literature [1,2]. In defining the rates we have implicitly

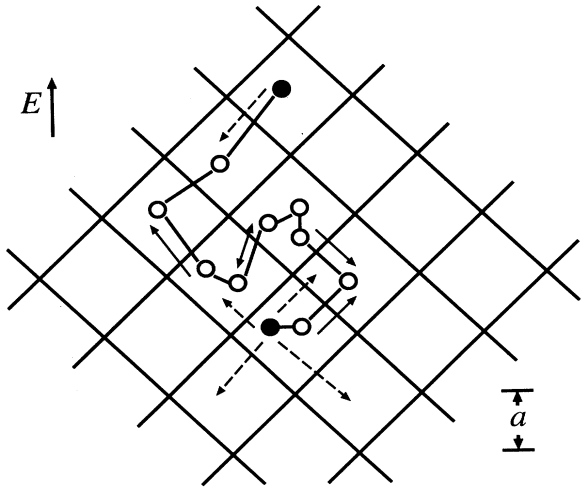

FIG. 1. The model of Rubinstein [3] as modified by Duke [4]. The circles denote subunits of the polymer, called reptons. The lines represent the segments of the polymer, which determine the shape of the polymer. The possible moves of the reptons are indicated by arrows. Internal moves can take place only in those cells in which there is more than one repton, or equivalently, when there are extra reptons (extrons) in a cell. The end points (solid circles) can make the moves indicated by the dashed arrows. The upper end point can only move back and shorten the chain as there is no extron in this cell. The lower end point has one extron, and the only external moves it can make is to grow. The reptons are noninteracting and all the possible moves are indicated. In the extron equilibrium model, the chain is fully characterized by the total number of reptons N (in this figure $N=11$), the length of the chain L (here $L=6$), and the shape of the polymer. As the shape in the direction perpendicular to the field E is not important, the shape is fully specified by the signs s_i of the individual segments, where $+1$ denotes up, and -1 denotes down. In this picture $s_i=\{1,1,-1,1,1,1\}$, where the index starts at the bottom segment. The number of extrons is $M=N-L-1=4$. While this picture is for $d=2$, we consider only the one dimensional projection along the field direction as the dimension only changes numerical prefactors.

*Present address: Department of Physics and Astronomy, Vrije Universiteit Amsterdam, De Boelelaan 1081, 1081 HV Amsterdam, The Netherlands.

assumed that $\epsilon < 1$ as for large fields effects such as hernia formation [5] takes place that are not taken into account in the model.

We distinguish between the moves by the end reptons (the external moves) and moves by the internal reptons. Internal moves can take place only when there is more than one repton in a given cell. We call these excess reptons extrons. Internal moves can be done only by extrons, and extrons can only make internal moves. Extrons are bosons since there is only one way to put n extrons in a given cell. In previous studies the internal reptons were taken to move with the same rates as the end points. This was done by computer simulations [6,7], and analytical approaches [8,9], usually for fairly low fields. Questions that were addressed were finite size corrections and possible scaling behavior [7,8].

In this paper we study the limit in which $W_i/W_e \to \infty$, so the end points are moving slowly compared to the internal reptons. The motivation for this is twofold: First, it is of relevance for those polymers that have special end groups, which can be heavy or large compared to the rest of the polymer. Second, it is a different model that has certain significant advantages for theoretical study as the importance of the end point motion is illustrated in its purest form. In this sense the results of this paper are complimentary to the results of Kooiman and van Leeuwen [9], who studied chains thus completely eliminating end point motion.

Models in which the stored length diffuses infinitely rapidly have been studied before [10,11]. However, the model introduced in this paper differs in one very important respect: fluctuations in the length of the polymer are taken into account. This first of all decouples the motion of the two ends of the polymer so that the dynamics are simpler and more physical. A second and more important consequence of this difference is that due to the fluctuations in the number of extrons, the drift velocity increases substantially, as shown below.

This paper is organized as follows. In Sec. II, the model is introduced. Next the behavior of long polymers is studied, where long means that the scaling parameter $N\epsilon^2 \gg 1$. In Sec. III, we calculate the drift velocity and in Sec. IV we present an approximate calculation of the average shape. Next, in Sec. V, we consider the crossover from the zero field behavior to the field dominated behavior. We demonstrate that another scaling variable, $N^3\epsilon^2$ determines this crossover. Some further aspects are pointed out in Sec. VI.

II. FAST EXTRON MODEL

In the limit $W_i/W_e \to \infty$ the extrons have time to equilibrate so we call this model the fast extron model (FEM). These transition rates are as follows. In order for the polymer to grow at the beginning of the chain, there must be at least one extron in this cell. We denote the number of extrons in cell number zero by n_0. There will be a certain probability $p(n_0>0)$ that there is at least one extron in the first cell. So for the growth rate for each of the $2d$ possible directions, we find ($W \equiv W_e$)

$$W_g = We^{\pm\epsilon/2} p(n_0>0) = We^{\pm\epsilon/2}(1-\theta_0) , \tag{2}$$

where the signs in the exponent depend on whether the chain grows up (+) or down (−), and $\theta_0 = p(n_0=0)$ is the probability that there is no extron in the first cell. In order for the chain to shrink, no extron must be present in cell 0, so that

$$W_s = We^{\pm\epsilon/2}\theta_0 , \tag{3}$$

where the sign in the exponent is determined by the first chain segment. The problem is now to establish the probability of finding no extrons at the end of the chain. As we consider the limit in which the extrons move infinitely fast, they have equilibrated and we can use equilibrium statistical mechanics to find this probability. θ_0 is then given by the ratio of two partition sums,

$$\theta_0 = \frac{Q'_{M,\{s_i\}}}{Q_{M,\{s_i\}}} , \tag{4}$$

where Q is the partition sum for M noninteracting bosons in a potential V_i, and Q' is the similar partition function in which there is no extron in the first cell. We describe the polymer shape by the segments s_i, which can be ± 1 depending on whether the segment is pointing up (+1) or down (−1) (see Fig. 1). Then the potential V_i is given by

$$V_i = \epsilon \sum_{j=i+1}^{L} s_j . \tag{5}$$

The potential is defined to be relative to the last cell i.e., $V_L = 0$. It is well known that the calculation of these canonical partition functions for bosons is complicated. We, therefore, use a grand canonical approach, in which the number of reptons is fluctuating, and only the average number of extrons is specified. In the grand canonical ensemble a chemical potential μ is introduced, which follows as the solution to

$$M = N - L - 1 = \sum_{i=1}^{L} \frac{1}{\exp(-\mu + V_i) - 1} . \tag{6}$$

There is no temperature prefactor in the exponent as this is already absorbed in the definitions of μ and V_i. In a simulation, Eq. (6) must be solved numerically. When we know the chemical potential, the transition rates averaged over the ensemble of extrons can easily be calculated. The probability that there is no extron at cell number zero is in the grand canonical ensemble

$$\theta_0 = 1 - e^{\mu + V_0} , \tag{7}$$

and the probability that there is no extron in the last chain cell is

$$\theta_L = 1 - e^{\mu} . \tag{8}$$

While these expressions appear to be asymmetric under the inversion of the polymer

$$\begin{aligned} i^* &= L - i , \\ s_i^* &= -s_{L-i+1} , \end{aligned} \tag{9}$$

they in fact do satisfy the symmetry as after transformation $\mu^* = \mu - V_0$, and $V_0^* = -V_0$.

It is possible to improve somewhat on the approximation made by using "almost canonical" transitions rates, and thereby suppress some of the fluctuations in the total number of reptons. From equilibrium statistical mechanics, we know the relation between the free energy A and the grand potential Ω

$$A = \Omega + \mu M \ . \tag{10}$$

As $Q = \exp(-A)$, this can be transformed into an approximate way to obtain the ratio of canonical partition sums, Eq. (4). Explicitly,

$$\theta_0 = \exp[\Omega - \Omega' + (\mu - \mu')M] \ , \tag{11}$$

with

$$\Omega = \sum_{i=1}^{L} \log(1 - e^{\mu - V_i}) \ . \tag{12}$$

Similarly in the primed expressions the term $i = 0$ is omitted. In a simulation, now three chemical potentials have to be calculated, μ and two μ's corresponding to both end cells. We found that for small ϵ there is hardly any difference between the probabilities calculated using the grand canonical ensemble, and the "almost canonical" transition rates. For large ϵ significant differences appear; for instance, configurations with very short chains occur much more frequently in the grand canonical simulation, which we believe to be an artifact of the use of the grand canonical ensemble. All the simulation results quoted are for "almost canonical" transition rates.

III. LONG CHAINS

In this and the next sections we consider the long chain limit. The crossover to short chains will be discussed in Sec. V. For long chains, a considerable simplification occurs: the motion of the polymer is such that there is a well defined head and a well defined tail, where the head is part of the polymer that is predominantly growing, and the tail is predominantly shrinking.

In the following, let s be the expectation value of s_i in the middle of the chain, which conventionally is taken to be positive. If we pick an arbitrary chain segment somewhere in the middle of the chain, (i.e., not close to the head or the tail) the probability that it will be up is $(1+s)/2$ and the probability that it will be a down segment is $(1-s)/2$. We use this in the following.

We first consider the expectation value of finding one extron at the end cells. As there are well defined heads and tails, this probability can be found by equating the growing rate of the head and the shrinking rate of the tail. At the head, the possible moves do not depend on each other, so we need to add up the rates. Denote the average orientation of the head segment by s_L. Then

$$\begin{aligned} R_{\text{head}} &= Wd(e^{\epsilon/2} + e^{-\epsilon/2})(1 - \theta_L) \\ &\quad - W\left[e^{\epsilon/2}\frac{1 - s_L}{2} + e^{-\epsilon/2}\frac{1 + s_L}{2}\right]\theta_L \\ &= W\cosh\frac{\epsilon}{2}\left[2d - \left[2d + 1 - \frac{s_L}{2}\tanh\frac{\epsilon}{2}\right]\theta_L\right] \ . \end{aligned} \tag{13}$$

We have used the convention that the head is at cell L, and the tail at cell 0. For the tail, all the segments have to be eliminated one after another and for the shrinking rate we need to add up the waiting times. As the polymer is long, V_0 is large and hence $\theta_0 \simeq 1$. If the tail is short, the value for s in the middle is also valid in determining the probabilities with which up and down segments arrive at the end. We then find

$$\begin{aligned} R_{\text{tail}} &= W\left[e^{-\epsilon/2}\frac{1 + s}{2} + e^{\epsilon/2}\frac{1 - s}{2}\right]^{-1} \\ &= W\left[\cosh\left[\frac{\epsilon}{2}\right]\right]^{-1}\left[1 - s\tanh\frac{\epsilon}{2}\right]^{-1} \ . \end{aligned} \tag{14}$$

In the stationary state $R_{\text{head}} = R_{\text{tail}}$ and this produces an expression for the probability θ_L in terms of s and s_L

$$\begin{aligned} \theta_L &= \left[2d + 1 - s_L\tanh\frac{\epsilon}{2}\right]^{-1} \\ &\quad \times \left\{2d - \left[\left[1 - s\tanh\frac{\epsilon}{2}\right]\cosh^2\frac{\epsilon}{2}\right]^{-1}\right\} \ . \end{aligned} \tag{15}$$

A more rigorous derivation, arriving at the same result, can be made by using the master equation and using a factorization assumption about correlations between subsequent segments [12]. For small fields, we do not need to know s as this would produce a higher order correction, and we find

$$R_{\text{head}} = W[2d - (2d+1)\theta_L] + O(\epsilon^2) \ , \tag{16}$$

irrespective of the value of s_L, and

$$R_{\text{tail}} = W + O(\epsilon^2) \ , \tag{17}$$

so that for low fields in the stationary state $\theta_L = (2d-1)/(2d+1)$. One first conclusion is that this probability does not depend on N, and is also nonvanishing. We note that for short chains and small fields $R_{\text{head}} = 0$ and $\theta_L = 2d/(2d+1)$. The average chemical potential of the long polymer we find, using Eq. (7), to be

$$\mu_0 = \log\frac{2}{(2d+1)} \ , \tag{18}$$

where the subscript zero reminds us that this is an average value over polymer shapes.

One of the most important quantities determining the shape of the polymer, as well as its drift velocity, is the average orientation of an internal segment s. This segment must have been formed at the head and its expectation value is given by

$$s=\frac{e^{\epsilon/2}p_s^+-e^{-\epsilon/2}p_s^-}{e^{\epsilon/2}p_s^++e^{-\epsilon/2}p_s^-}\ , \tag{19}$$

where $p_s^\pm$ is the probability that an up (+) or down (−) segment survives to make it to the interior.

A simple estimate for s is used in the biased reptation model [13]. There it is assumed that a segment, once formed, stays forever, so that $p_s^\pm=1$. Extending this line of thought to the fast extron model results in

$$s^{(\mathrm{BRM})}=\tanh\left[\frac{\epsilon}{2}\right]\ . \tag{20}$$

This argument does not give the average orientation observed in simulations. What is ignored is that chain segments, once formed, can again be wiped out by a subsequent shrinking of the head. As for low fields $\theta_L=(2d-1)/(2d+1)$, this has a nonvanishing probability and must be taken into account. For the Rubinstein-Duke model, this was first pointed out by Duke, Semonov, and Viovy [14].

In the FEM, the staying probability can be fairly accurately calculated with the following argument that can be called "one cell deep." Let us assume that the most recently grown segment at the head was up. The probability q^+ that this segment will be wiped out on the next move of the head segment of the polymer is the rate with which the polymer shrinks divided by the total rate of changing the end repton

$$q^\pm=\frac{\theta_L^\pm e^{\mp\epsilon/2}}{\theta_L^\pm e^{\mp\epsilon/2}+d(1-\theta_L^\pm)(e^{\epsilon/2}+e^{-\epsilon/2})}\ , \tag{21}$$

where $\theta_L^+=\theta_L(s_L=1)1-e^{\mu+}$, with $\mu^+\equiv\mu(s_L=1)$ the chemical potential with the last chain segment up. When the last segment happens to be down, we have a similar q^- with chemical potential μ^-. The probabilities for the segments surviving one move are $1-q^+$ and $1-q^{-1}$ for up and down segments, respectively. These probabilities are of the order of $4d/(6d-1)$ for low fields. Since this probability is high, we now assume that if the segment survive one move, they will stick forever

$$p_s^\pm=1-q^\pm\ . \tag{22}$$

This does not give s directly as it requires $\mu(s_L=\pm1)$. For low fields, the chemical potential $\mu^\pm$ will be close to μ^0. The thermodynamic potential in all the cells except for the last cell (i.e., $\mu-V_i$) will be influenced only slightly $O(\epsilon^2)$ by the orientation of the last segment, as for low fields the extrons can be on many sites. However, by definition the chemical potential is defined relative to the last cell. So the chemical potential will depend on the orientation of the last cell, and $\mu^\pm\simeq\mu^0\epsilon$, where μ^0, is the average chemical potential, Eq. (18). This is substantiated below, Eq. (46). With these $\mu^\pm$, we obtain

$$s=\frac{6d}{6d-1}\epsilon\quad(\epsilon\ll1)\ . \tag{23}$$

For low fields, we can improve on the approximation implied in Eq. (22). For low fields we can assume that the $q^\pm$ do not depend on the specific path taken. We can then calculate the probability that the newly formed segment will not only survive its first subsequent jump, but *all* subsequent jumps. This is found to be [15]

$$p_s^\pm=\frac{1-2q^\pm}{1-q^\pm}\ . \tag{24}$$

This yields a different estimate for the s, which should be more accurate than Eq. (23) for low fields. Using again that for low fields $\mu^\pm\simeq\mu^0\pm\epsilon$, we obtain

$$s=\frac{1+4d}{1+2d}\epsilon\quad(\epsilon\ll1)\ . \tag{25}$$

As is demonstrated in Fig. 2, this produces a good agreement with the simulation results for the low field value of s. The argument cannot be extended to higher fields as then the assumption that q is independent of the last few segments can no longer be justified.

The average drift velocity can now easily be calculated as

$$v=s\langle u_c\rangle a\ , \tag{26}$$

where $\langle u_c\rangle$ is the average curvilinear velocity, or the average rate with which the extrons are transported along the chain. This curvilinear velocity clearly is equal to the rate at which extrons are put into the polymer at the end, so $\langle u_c\rangle=R_{\mathrm{tail}}$ and hence

$$v=\frac{sWa}{\cosh\frac{\epsilon}{2}\left[1-s\tanh\frac{\epsilon}{2}\right]}\ . \tag{27}$$

The only nontrivial quantity here is s. For low fields, we find

$$v=\frac{1+4d}{1+2d}\epsilon Wa\ . \tag{28}$$

Extending the ideas of the biased reptation model [cf. Eq. (20)] would have resulted in $v=\epsilon Wa/2$. Our result is

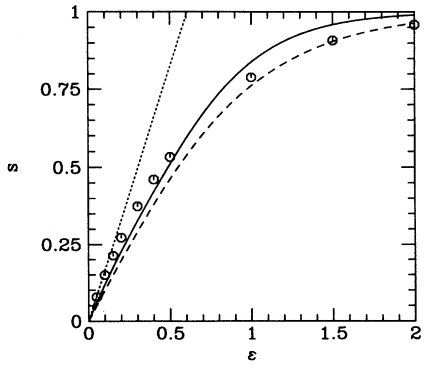

FIG. 2. The average value of s in the interior of the polymer. This number determines the average end point distance along the field S as $S\simeq Ns$. The circles are simulation results, the solid line is the analytic prediction Eq. (19) using the chemical potentials from Eq. (60), the dotted line is the low field result Eq. (25), and the dashed line is the high ϵ result Eq. (31).

larger by a factor 10/3 in one dimension.

For large fields $\epsilon \gtrsim 1$; on the other hand the chemical potential μ^+ and μ^- differ. When the last chain segment is up, many extrons move to this newly formed cell, and hence the chemical potential changes substantially

$$\mu^+ \simeq \mu^0 . \tag{29}$$

But, with the last segment down, only a few extrons move to this cell and the chemical potential changes little

$$\mu^- \simeq \mu^0 - \epsilon . \tag{30}$$

This results in

$$s = 1 - \frac{2}{e^{2\epsilon}+1} \quad (\epsilon \gtrsim 1) \tag{31}$$

and

$$v = Wa \sinh\epsilon . \tag{32}$$

Equation (31) is compared to simulation results in Fig. 2. In Fig. 3, the drift velocity of the long polymer is presented as a function of the electric field. A remarkable and for us unexpected result is that v/ϵ has an initial *decrease* with ϵ. For low fields, simulation results for the drift velocity seem to converge to the low field value implied by Eq. (28).

IV. SHAPE OF LONG POLYMERS

We first estimate the average number of extrons in the chain. As extrons are bosons, we have

$$\begin{aligned} M &= \sum_i \frac{1}{\exp(-\mu - V_i) - 1} \\ &\simeq \int_0^\infty dx \frac{1}{\exp(-\mu + sx\epsilon) - 1} \\ &= -\frac{1}{s\epsilon} \log(1 - e^{\mu}) , \end{aligned} \tag{33}$$

where we have replaced the sum by an integral, and we have assumed that deviations of V_x from its average value $sx\epsilon$ are small. Using Eq. (18) and $s = (4d+1)\epsilon/(2d+1)$ for low fields [Eq. (25)], we obtain for the average number of extrons

$$\langle M \rangle \simeq \frac{(2d+1)}{(4d+1)\epsilon^2} \log\left[\frac{2d+1}{2d-1}\right] . \tag{34}$$

This expression can only be expected to be reasonable when the number of extrons is large, or equivalently, the applied field is low. The most important conclusion is that M is independent of N. As $L = N - M - 1$, the chain is completely stretched except for an ϵ dependent number. This conclusion agrees with simulation results. The convergence of any property of the polymer with N is quite slow, if we consider, for example, the not-very-small field $\epsilon = 0.1$, then $M \simeq 66$ in one dimension. This must be a small fraction of the total number of reptons, so the long chain limit applies only for $N \gtrsim 2000$ for $\epsilon = 0.1$. In Fig. 4, simulation results for the number of extrons are presented. The simulations are compatible with the ϵ^{-2} dependence of the number of extrons, but the numerical prefactor is found to be about 2.1 times larger for the almost canonical transition rates, and the prefactor is about five times larger for the grand canonical transition rates. A better estimate for the number of extrons is presented below, Eq. (47).

Next we consider the average shape of the polymer, for which we present a typical simulation result in Fig. 5. For the tail, we have found a successful argument describing the results. In simulations we found that only the single last segment of the tail has a different orientation than the middle of the chain. An analytic argument that gives satisfactory results is to take the average of the possibilities that the segment is up or down, weighed by

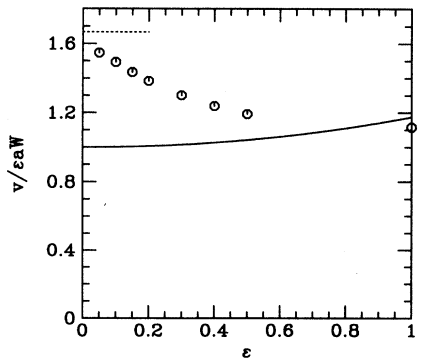

FIG. 3. The drift velocity divided by the applied field. The circles are simulation results, the solid line is the analytic prediction Eq. (32), and the dotted line is the low field prediction Eq. (28).

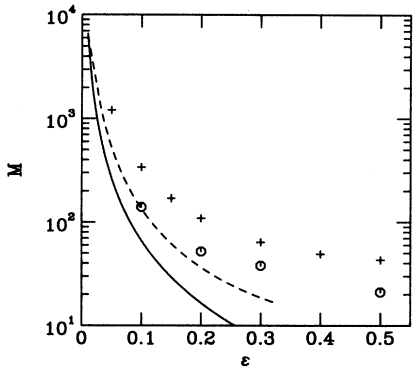

FIG. 4. The average number of extrons in a long polymer as a function of the applied field ϵ. We found that this number is independent of the total number of reptons N, as long as $N\epsilon^2 \gg 8$. The circles are simulation results for the "almost canonical" transition rates, the pulses are simulation results for the grand canonical transition rates, and the solid line is the analytic prediction Eq. (34). The dashed line is the number of extrons following from the polymer shape as calculated in Sec. IV, Eq. (47). The number of extrons is the *only* quantity that depends on the specific simulation technique. Other results differed by less than 1%.

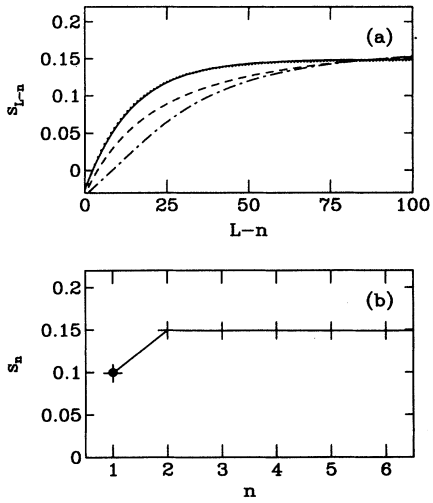

FIG. 5. The average shapes of the head (a) and the tail (b) for $\epsilon=0.1$ and $N=2000$. For these parameters $s=0.15$. The simulation results are dots in (a), and pulses in (b). The solid line is an exponential in (a), and a guide to the eye in (b). While for the tail only the last segment is different from the middle part of the chain, the head shape can be accurately represented by an exponential. The dashed line in (a) is the first order analytic prediction Eq. (48), whereas the dot-dashed curve is the converged solution of the set of equations described in Sec. IV. The black dot in (b) is the prediction of Eq. (35) using the simulation value for s.

the waiting times when it is up or down. This results in

$$\langle s_1\rangle=\frac{s-\tanh(\epsilon/2)}{1-s\tanh(\epsilon/2)}\ . \tag{35}$$

This expression we found to be accurate, see Fig. 5(b). It is consistent with Eq. (14) in that an alternative derivative of the shrink rate consists of adding properly weighed shrink rates, which would yield Eq. (14). The derivation of Eq. (35) can be made more precise by using the master equation [12].

For the shape of the head, the analogous argument is more complicated. We assume that the shape can be understood by a similar time argument, i.e., if certain segment n happens to be up, there will be slightly higher than average number of extrons in the last cell, causing the chain to grow slightly more rapidly than average. Conversely if this particular segment happens to be down, the polymer will grow somewhat slower. The result is that the probability of finding the nth segment down is enhanced compared to its value in the middle. Explicitly

$$\langle s_n\rangle=\frac{(1+s)T_n^+-(1-s)T_n^-}{(1+s)T_n^++(1-s)T_n^-}\ , \tag{36}$$

where we are interested in n close to L, i.e., $L-n$ is small. As we are interested mainly in the small field limit, this can be simplified to

$$\langle s_n\rangle=s+\frac{T_n^+-T_n^-}{T_n^++T_n^-}\ , \tag{37}$$

where $T_n^{\pm}$ is the average time that it takes for the polymer to grow a new segment or wipe out one segment when the nth segment happens to be up $(+1)$ or down (-1). Taking the average over all the segments except for the nth and using Eq. (13), we find the growth rate

$$T_n^{\pm}=R_{\text{head}}^{-1}(s_n=\pm1)$$
$$=\frac{1}{W}\{(2d+1)\exp[\mu(s_n=\pm1)]-1\}^{-1} \tag{38}$$

for $n<L$. As is evident from Eq. (13), $n=L$ is special and we obtain

$$T_L^{\pm}=\frac{1}{W}\left[(2d+1)\exp\left[\mu(s_L=\pm1)\mp\frac{\epsilon}{2}(1-\theta_L)\right]-1\right]^{-1}. \tag{39}$$

We next assume that dependence of the chemical potential on the orientation of the nth segment is given by a linear combination

$$\mu=\mu_0+\sum_{n=1}^{L}\mu_n(s_n-\langle s_n\rangle)\ , \tag{40}$$

where $\mu_n\propto\epsilon$, and moreover, μ_n is small when n is not close to L. As $\mu_0=\log[2/(2d+1)]$, and μ_n is small

$$\langle s_n\rangle=s-2\mu_n \tag{41}$$

and

$$\langle s_L\rangle=s-2\mu_L+\epsilon\frac{2d-1}{4d+2}\ . \tag{42}$$

To find μ_n, we assume that the number of extrons is independent of the orientation of the last few segments. In reality, the number of extrons will fluctuate, and μ_n is hard to determine. To assume that the number of extrons is a constant is a physical assumption, which has to be checked *a posteriori*. Using Eq. (6), putting $dM/ds_n=0$, and assuming that fluctuations in the potentials are small, we obtain

$$\mu_n=\epsilon\frac{\Xi_{n-1}}{\Xi_L}\ , \tag{43}$$

with

$$\Xi_n=\sum_{i=0}^{n}\frac{\exp(-\mu_0+\bar V_i)}{[\exp(-\mu_0+\bar V_i)-1]^2}\ , \tag{44}$$

where $\bar V_i$ is the average potential at cell i,

$$\bar V_i=\epsilon\sum_{j=i}^{L}\langle s_j\rangle\ . \tag{45}$$

Note that we have

$$\mu_L=\epsilon\ , \tag{46}$$

which we have used in Sec. III. Given the $\langle s_n\rangle$, we can find an estimate for the number of extrons, which is more accurate than Eq. (34),

$$M=\sum_{i=0}^{L}\frac{1}{\exp(-\mu_0+\bar V_i)-1}\ . \tag{47}$$

We have a closed set of equations for $\langle s_n \rangle$ and μ_n that can be solved, for instance, by iteration. The solution is presented in Fig. 5. In the first iteration, we can put $\langle s_n \rangle = s$ in the calculation of $\bar{V}_i$ to obtain

$$\mu_{L-n} = \epsilon \frac{1}{2e^{ns\epsilon} - 1} . \tag{48}$$

This expression is also presented in Fig. 5. There is a semiquantitative agreement between this expression and the simulation results. Equation (25) gives a value for the penetration depth

$$H \simeq \frac{1}{s\epsilon} = \frac{2d+1}{4d+1} \frac{1}{e^2} . \tag{49}$$

Simulation results suggest an $\epsilon^{-3/2}$ dependence for H as is demonstrated in Fig. 6.

V. CROSSOVER TO THE VERY LOW FIELD BEHAVIOR

We have firmly established the picture that there is a well defined head and a well defined tail for long chains. This assumption is expected to break down when the number of extrons that follows from Eq. (34) becomes comparable to the number of extrons present in a polymer in zero field, $M = N/(2d+1)$. In one dimension this happens when $N\epsilon^2 < 8$. While something will happen for $N\epsilon^2 \sim 1$, we found that there is a crossover to low fields taking place at much smaller fields. For zero fields $\theta_0 = 2d/(2d+1)$, and in simulations we found that corrections are of the order of $\epsilon\sqrt{N}$. In this section, we will only consider field so small that $\theta_0 \simeq 2d/(2d+1)$.

We focus on the renewal time t_r, the time which is needed for all the segments of the polymer to be renewed. To this end we consider the related quantity, the curvilinear velocity correlation function,

$$\Phi(t) = \langle \mu_c(0) u_c(t) \rangle . \tag{50}$$

Here u_c is defined as the center-of-mass velocity along the segment index. Equivalently, it is half the number of segments grown per unit time on one end minus half the number of segments grown per unit time on the other end. The curvilinear velocity is a fluctuating quantity, i.e., it is either zero or very large for a very short time. This is to be contrasted with the grow and shrink rates of Sec. III, where we were interested in the average value of the curvilinear velocity. We are interested in average properties, which are defined as time averages, or equivalently, stationary state averages. The velocity correlation function has two physically different contributions, a δ-function contribution due to the hopping of the end points, and a slowly decaying contribution that is due to the applied field. The δ-function contribution is due to uncorrelated subsequent jumps of the end reptons. The rate with which the two end reptons jump is $2W[2d-(2d-1)\theta_0] = 8dW/(2d+1)$ as $\theta_0 = 2d/(2d+1)$.

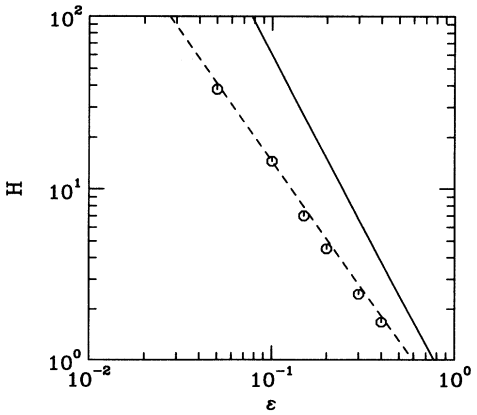

FIG. 6. The penetration depth H as a function of the applied field. The circles are simulation results and the solid curve is the analytic prediction $H = 3/5\epsilon^2$, Eq. (49). The dashed line is the curve $H = 14.5(10\epsilon)^{-3/2}$, and is a fit to the simulation results.

The physical origin of the slowly decaying contribution can be understood by noting that the end-to-end vector along the field changes only on the renewal time scale. At a given time, the average curvilinear velocity is proportional to half of the growth rate at one end minus half the growth rate at the other end. As we are considering small fields we can linearize the dependence on V in Eqs. (7) and (13). For the average curvilinear velocity, constrained by the value of the end-to-end vector S, we find

$$\langle u_c \rangle_S = \frac{2d+1}{2} W[\theta_0 - \theta_L] = \frac{W\epsilon S}{2} . \tag{51}$$

Therefore, the initial value of the slowly decaying component is equal to the average of the square of the curvilinear velocity, $\langle u_c \rangle_S^2$. We thus have

$$\Phi(t) = \frac{d}{2d+1} W\delta(t-0^+) + \frac{L}{4} W^2\epsilon^2 g(t) , \tag{52}$$

where the prefactor to the δ-function contribution is reduced by a factor of 4 as we consider the center-of-mass motion, and by an additional factor of 2 due to the convention $\delta(t) = [\delta(t-0^+) + \delta(t-0^-)]/2$. We have also used that $\langle S^2 \rangle = L$.

The function $g(t)$ can be calculated fairly accurately. According to Eqs. (51) and (52), we have

$$g(t) = \frac{1}{L} \langle S(0)S(t) \rangle = \frac{1}{L} \sum_{n=1}^{L} \langle s_n(0) s_n(t) \rangle \tag{53}$$

since in the zero field limit segments are uncorrelated and any newly formed segment will be uncorrelated with the earlier formed segments. For a particular segment, n one has $s_n(t) = s_n(0)$ as long as it is not eliminated from the chain by either of the two ends. If it later might reemerge, $s_n(t)$ is uncorrelated to s_n and, therefore, on the average zero. As the ends of the polymer move randomly to segment n, the calculation of the survival probability is a standard problem of random walks. We consider a slightly different problem and let the segment n randomly wander in the chain of fixed length L till it escapes from the boundaries. The reason for doing so is that the end points move correlated such as to keep the chain at fixed length L. When it shrinks, the extron number increases

and, therefore, the tendency to grow increases and vice versa. The random walker escaping from a fixed region is a simpler problem and yields the following solution for $g(t)$

$$g(t)=\frac{2}{L^2}\sum_{k=1,3\ldots}^{L}\left[\operatorname{cotan}\frac{\pi k}{2(L+1)}\right]^2 \times\exp\left[-2\left[1-\cos\frac{\pi k}{L+1}\right]\frac{dWt}{2d+1}\right]. \tag{54}$$

This expression has a delicate behavior for times of order unity. However, for short times the assumption of constant length is not valid. The interesting behavior of this expression is for times of order L^2. Then the cotangent and cosine in Eq. (54) can be expanded to yield the rapidly converging series

$$g(t)=\frac{8}{\pi^2}\sum_{k=0}^{\infty}\frac{1}{(2k+1)^2}\exp\left[-\frac{(2k+1)^2\pi^2 dWt}{(2d+1)L^2}\right] =\frac{8}{\pi^2}\left[e^{-\tau}+\tfrac{1}{9}e^{-9\tau}+\tfrac{1}{25}e^{-25\tau}+\cdots\right], \tag{55}$$

where we used the shorthand $\tau=\pi^2 dWt/(2d+1)L^2$. This approximation gives the correct initial value $g(t=0)=1$, but fails to give the proper initial slope. The resulting velocity correlation function is plotted in Fig. 7, and agrees very well with simulation results for low fields.

Clearly, the polymer renews itself on the time for which one of the end reptons has an average curvilinear displacement of $L=2dN/(2d+1)$, or rather a mean square displacement of L^2. In terms of the velocity correlation function, the renewal time t_r is the solution of the equation

$$L^2=\int_0^{t_r}dt_1\int_0^{t_r}dt_2\Phi(|t_2-t_1|) =2\int_0^{t_r}dt(t_r-t)\Phi(t). \tag{56}$$

As $g(t)$ is rapidly decaying, we can extend the integral to long times. When we ignore the contribution proportional to $t\Phi(t)$, this results in

$$t_r=\frac{2d}{2d+1}\frac{1}{W}\frac{N^2}{1+dN^3\epsilon^2/6(2d+1)}. \tag{57}$$

A remarkable feature of this result is that there is a crossover where the applied field is of relevance for $N^3\epsilon^2\sim 6(2d+1)/d$, so the scaling parameter determining this crossover is $N^{3/2}\epsilon$. This is to be compared to the scaling parameter of the previous sections, $\epsilon N^{1/2}$. For the Rubinstein-Duke model, the scaling parameter that determines whether the applied field significantly changes the physics is believed to be $N\epsilon$ [7]. The fast extron model is apparently even more susceptible to perturbations. A crossover behavior with scaling parameter $N^3\epsilon^2$ has been found before for the biased reptation model [16–18]. This crossover is of the same nature as the one found here as it describes the change of the polymer renewal time with applied field.

When the applied field is increased, the calculation given for $g(t)$ no longer applies. In the calculation we had assumed that the center-of-mass performs a simple diffusive motion, whereas we have just shown that for $N^3\epsilon^2\sim 18$ the renewal time, and therefore the center-of-mass motion, is significantly affected by the field. In Fig. 8, we show that $t_r<2N^2/3W$ for larger values of $N^3\epsilon^2$, an observation we return to in the discussion.

The mobility coefficient in the zero field limit is found by using Eq. (57) and the relation $\langle\Delta R^2\rangle=a^2\langle S^2\rangle=a^2L$,

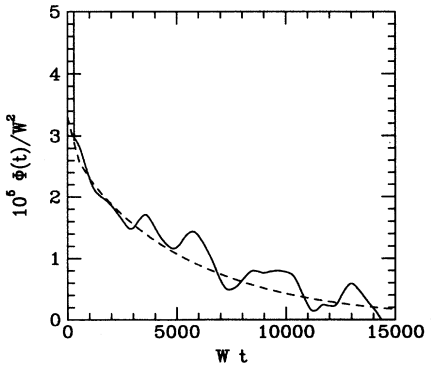

FIG. 7. The velocity correlation function $\Phi(t)$ (solid) for $N=200$, $\epsilon=0.001$ compared to the analytic expression Eq. (52). The wiggles are simulation noise.

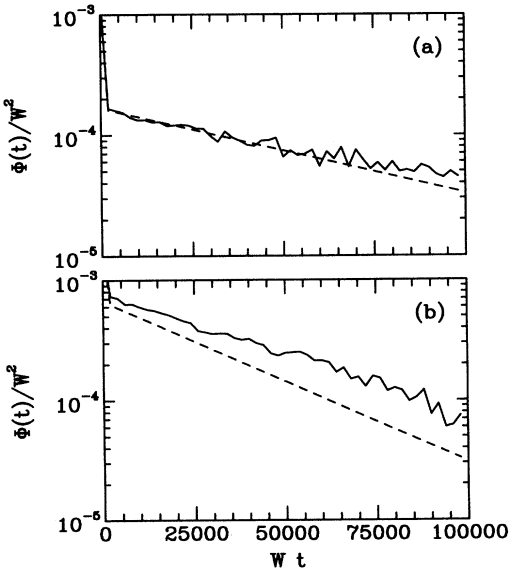

FIG. 8. (a) The velocity correlation function $\Phi(t)$ (solid) for $N=1000$, $\epsilon=0.0005$. Apart from the remnant of the δ peak at $t=0$, we find a slowly decaying contribution. The dashed line is the exponential Eq. (52) with a decay time $W/\lambda=61853$, which is the decay time $t_r/2$ given by Eq. (63). In this figure the simulation extended over 2×10^8 steps. (b) $\Phi(t)$ (solid) for $N=1000$, $\epsilon=0.001$ compared to the exponential Eq. (52) with a decay rate λ given by Eq. (63), $W/\lambda=32553$. In (a) $N^3\epsilon^2=250$, and in (b) $N^3\epsilon^2=1000$.

$$\mu = Nq\frac{\langle \Delta R^2 \rangle}{2t_r} = a^2 qW \ . \tag{58}$$

The derivation presented here gives another understanding why the scaling is different from $N\epsilon^2$, as might have been expected on the basis of the results of the previous sections. While a specific configuration of the polymer has a small curvilinear velocity proportional to $N\epsilon^2$, it will keep its orientation for a very long time, of the order of N^2. There is an important difference of the fast extron model and the Rubinstein-Duke (RD) model in that in the FEM the head and tail flip after essentially one renewal, whereas this will be a much slower process in the RD model.

VI. DISCUSSION

In Sec. III, we have presented results for the average orientation of the polymer in the low ϵ and high ϵ regimes. To interpolate between these two cases, we use the sticking probabilities Eq. (22). While for low fields the chemical potentials $\mu^+ = \mu^-$, this no longer holds for elevated fields as is already demonstrated in Eqs. (29) and (30). For intermediate fields, the chemical potentials lie in between these cases. The chemical potentials μ^0, immediately before the last grow, follows from Eq. (7)

$$\mu^0 = \log[1-\theta_L] \ . \tag{59}$$

The chemical potentials $\mu^{\pm}$ can be found by requiring that these potentials are compatible with the number of extrons M. This is not an exact calculation, as in reality M will fluctuate. Keeping the first term in Eq. (33) explicitly, assuming that M is constant results in

$$\log(1-e^{\mu^0}) = \log(1-e^{\mu^{\pm}}) - \frac{s\epsilon}{[1-\exp(\pm\epsilon+\mu^{\pm})]} \ . \tag{60}$$

We now have a closed set of equations. The numerical solution of the set of equations (19), (59), and (60) is presented in Fig. 2. The approximations made cannot really be justified for higher fields, in particular the validity of Eq. (33) is doubtful. Yet, Eq. (31) remains valid for large fields.

In Sec. V, we have seen that the curvilinear velocity decay rate decreases with $N^3\epsilon^2$. We can make this quantitative if we assume that for all fields the velocity correlation function is a single exponential. The motivation for this is that Eq. (55) shows that by far the largest contribution to g is from the $k=0$ contribution. So we assume (we take the one dimensional case from now on)

$$\Phi(t) = \tfrac{1}{3}W\delta(t-0^+) + \frac{N}{6}W^2\epsilon^2 e^{-\lambda t} \ . \tag{61}$$

This assumption actually works well for $N^3\epsilon^2$ up to 1000 as illustrated in Fig. 8. For low fields we have $\lambda = 3\pi^2/4N^2$ [see Eq. (55)]. Clearly it is to be expected that λ is of the order of $1/t_r$. For large fields, we found that good results are obtained if we assume that $\lambda \simeq 2/t_r$. This leads to the following equation for t_r:

$$\tfrac{2}{3}Wt_r + \frac{NW^2\epsilon^2}{12}\alpha t_r^2 = \tfrac{4}{9}N^2 \ , \tag{62}$$

with $\alpha = 1+e^{-2}$. The solution of Eq. (62) is

$$t_r = \frac{4}{\alpha WN\epsilon^2}\left[\left[1+\frac{\alpha N^3\epsilon^2}{3}\right]^{1/2} - 1\right] \ . \tag{63}$$

We find that the renewal time decreases with the applied field, smoothly crossing over from

$$t_r = \frac{2N^2}{3W} \quad \left[\epsilon^2 \ll \frac{1}{N^3}\right] \ , \tag{64}$$

to

$$t_r = \frac{4}{\epsilon W}\left[\frac{N}{\sqrt{3\alpha}}\right]^{1/2} \quad \left[\frac{1}{N^3} \ll \epsilon^2 \ll \frac{1}{N}\right] \ . \tag{65}$$

As is illustrated in Fig. 8, Eq. (63) is quite accurate for $N^3\epsilon^2$ up to about 1000. This observation suggests that the crossover behavior described by Eq. (63) correctly describes the dynamics, and is an argument that the low field phase and the intermediate phase where the tube renewal is determined by the field are smoothly connected to each other. For large values of $N^3\epsilon^2$, the curvilinear velocity correlation function is observed to be systematically larger than the prediction of Eq. (61); the onset of this trend is already visible in Fig. 8(b). Renewal times obeying scaling laws similar to Eq. (63) were found for the biased reptation model [16,17]. In these articles also the consequences for the mobility were discussed.

ACKNOWLEDGMENTS

This work was supported by Stichting voor Fundamenteel Onderzoek der Materia (FOM), which is financially supported by the Nederlandse Organisatie voor Wetenschappelijk Onderzoek (NWO). We thank Jeroen Balkenende for useful discussions and for his careful reading of the manuscript.

[1] P. G. de Gennes, J. Chem. Phys. **55**, 572 (1971).
[2] M. Doi and S. F. Edwards, *The Theory of Polymer Dynamics* (Oxford University Press, Oxford, 1986).
[3] M. Rubinstein, Phys. Rev. Lett. **59**, 1946 (1987).
[4] T. A. J. Duke, Phys. Rev. Lett. **62**, 2877 (1989).
[5] J. M. Deutsch, Phys. Rev. Lett. **59**, 1255 (1987).
[6] T. A. J. Duke, J. Chem. Phys. **93**, 9049 (1990).
[7] G. T. Barkema, J. F. Marko, and B. Widom, Phys. Rev. E **49**, 5303 (1994).
[8] B. Widom, J. L. Viovy, and A. D. Désfontaines, J. Phys. (France) I **1**, 1759 (1991).
[9] J. M. J. van Leeuwen and A. Kooiman, Physica A **184**, 79 (1992); A. Kooiman and J. M. J. van Leeuwen, *ibid.* **194**, 163 (1992); J. Chem. Phys. **99**, 2247 (1993); A. Kooiman, Ph.D. thesis, University of Leiden, 1993.
[10] G. W. Slater, J. Phys. (France) II **2**, 1149 (1992).

[11] O. Lumpkin, S. D. Levene, and B. H. Zimm, Phys. Rev. A **39**, 6557 (1989).
[12] J. Balkenende, J. A. Leegwater, and J. M. J. van Leeuwen, in *25 Years of Kinetic Theory* (Springer-Verlag, Berlin, 1995).
[13] O. J. Lumpkin, P. Déjardin, and B. H. Zimm, Biopolymers **24**, 1573 (1985); G. W. Slater and J. Noolandi, *ibid.* **25**, 431 (1986).
[14] T. A. J. Duke, A. N. Semenov, and J. L. Viovy, Phys. Rev. Lett. **69**, 3260 (1992).
[15] N. G. Van Kampen, *Stochastic Processes in Physics and Chemistry* (North-Holland, Amsterdam, 1981).
[16] J. L. Viovy, Biopolymers **26**, 1929 (1987).
[17] G. W. Slater, Electrophoresis **14**, 1 (1993).
[18] G. W. Slater, P. Mayer, and G. Drouin, Electrophoresis **14**, 961 (1993).